Magnetic Resonance in Medicine 49:1019–1027 (2003)

Microvascular BOLD Contribution at 4 and 7 T in the Human Brain: Gradient-Echo and Spin-Echo fMRI With Suppression of Blood Effects

Timothy Q. Duong,* Essa Yacoub, Gregory Adriany, Xiaoping Hu, Kâmil Uğurbil, and Seong-Gi Kim

The BOLD signal consists of an intravascular (IV) and an extravascular (EV) component from both small and large vessels. Their relative contributions are dependent on field strength, imaging technique, and echo time. The IV and EV contributions were investigated in the human visual cortex at 4 and 7 T using spin-echo and gradient-echo BOLD fMRI with and without suppression of blood effects. Spin-echo acquisition suppresses EV BOLD from large veins and reflects predominantly blood T_2 changes and EV BOLD signal from small blood vessels. At a short echo time (32 ms), diffusion gradient-based suppression of blood signals resulted in a 75% and 20% decrease in spin-echo BOLD changes at 4 T and 7 T, respectively. However, at echo times (55–65 ms) approximating tissue T_2 typically used for optimal BOLD contrast, these gradients had much smaller effects at both fields, consistent with the decreasing blood T_2 with increasing field strength. Gradient-echo BOLD percent changes, with relatively long echo times at both fields, were virtually unaffected by gradients that attenuated the blood contribution because the EV BOLD surrounding both large and small vessels dominated. These results suggest that spin-echo BOLD fMRI at 4 and 7 T, with TE approximating tissue T_2, significantly reduces nonspecific mapping signals from large vessels and significantly accentuates microvasculature contributions. Magn Reson Med 49:1019–1027, 2003.

Key words: spatial specificity; brain mapping; high magnetic fields; diffusion-weighting

From its inception approximately a decade ago, functional MRI (fMRI) based on blood oxygenation level-dependent (BOLD) contrast has become the most commonly used methodology for mapping brain function. Virtually all of these studies have been performed in the spatial scale of several millimeters to a centimeter in humans. Extending these efforts to higher spatial resolution (millimeter to submillimeter) functional mapping requires delineating the exact vascular source of the fMRI signals because BOLD contrast is dependent on blood-vessel diameter, magnetic field strength (B_0) and image acquisition methods (e.g., Hahn spin-echo (HSE) vs. gradient-echo (GE)) (1,2). The BOLD effect arising from the capillary bed can be expected to have the same spatial extent as perfusion and oxygen consumption rate increases induced by increased synaptic activity (3). On the other hand, functional maps based on BOLD effects originating from the larger diameter draining veins can be significantly distant from the actual site of neuronal activity. Therefore, minimizing the macrovascular contribution is critical for high-resolution fMRI.

The BOLD signal consists of an intravascular (IV) and an extravascular (EV) component, both of which can arise from small and large blood vessels (1,2,4–9). The EV effects from large vessels can be eliminated with HSE methods because the 180° RF pulse refocuses the static dephasing induced by field inhomogeneities around large vessels. The IV BOLD component exists because blood deoxyhemoglobin content strongly influences the T_2 and T_2^* of blood, as well as the susceptibility-induced frequency difference between blood and surrounding tissue. Both mechanisms contribute to blood-related signals in GE fMRI. In HSE-based fMRI, the second mechanism is not operative; nevertheless, IV effects persist in HSE fMRI because the blood T_2 is dependent on the blood-oxygenation state. The IV effect originates from venous vessels of all sizes and is a potential source of inaccurate "activation" signals.

The IV contribution to the BOLD response can be examined using Stejskal-Tanner (S-T) gradients (10), commonly referred to as bipolar gradients. S-T gradients induce diffusion-dependent signal loss and were in fact first used for studying diffusion (10). These gradients induce velocity-dependent phase shifts in the presence of flow. Consequently, they can suppress signals from moving blood because of inhomogeneous velocities within a vessel and the presence of blood vessels of different orientations within a voxel. The latter mechanism is the basis for the intravoxel-incoherent-motion (IVIM) phenomenon (11). In addition to the flow/IVIM effects, the S-T gradients also suppress tissue signals, although to a lesser extent because the apparent water diffusion is slower in tissue relative to blood. Cognizant of the multiple effects of S-T gradients, we will refer to these gradients as IVIM gradients herein for simplicity. In the presence of these IVIM gradients the BOLD fMRI signals at 1.5 T were reported to have either disappeared completely (12) or reduced by ~70% (13). These studies concluded that at 1.5 T BOLD fMRI signals arise predominantly from effects associated with blood in

Center for Magnetic Resonance Research, Department of Radiology, University of Minnesota School of Medicine, Minneapolis, Minnesota.

Grant sponsor: NIH; Grant numbers: RR08079; NS38295; NS40719; EB00331; S10 RR13957; Grant sponsor: NSF; Grant number: DBI 9907842; Grant sponsors: MIND Institute; W.M. Keck Foundation.

Timothy Q. Duong's current address is Center for Comparative NeuroImaging, Department of Psychiatry University of Massachusetts Medical School, Worcester, MA 01655.

Xiaoping Hu's current address is the W.H. Coulter Dept. of Biomedical Engineering, Emory University, Atlanta, GA 30322.

Seong-Gi Kim's current address is Department of Neurobiology, University of Pittsburgh Medical School, Pittsburgh, PA 15261.

*Correspondence to: Timothy Duong, Ph.D., Center for Comparative NeuroImaging, University of Massachusetts Medical School, 55 Lake Ave. N, Worcester, MA 01655. E-mail: timothy.duong@umassmed.edu

Received 15 May 2002; revised 10 February 2003; accepted 12 February 2003.

DOI 10.1002/mrm.10472
Published online in Wiley InterScience (www.interscience.wiley.com).

large venous vessels. A similar conclusion was reached for 1.5 T using other approaches (8,14).

The IV BOLD effect should diminish with increasing magnetic field due to the shortening of blood T_2 or T_2^* relative to tissue T_2 or T_2^* at high fields (15). This was documented at 9.4 T in the anesthetized rat model (7,16). However, the vascular source of the BOLD effect at high fields in humans remains unknown. In the present study, the IV and EV contributions to HSE and GE large venous vessels to the BOLD functional maps in human visual cortex were investigated at 4 and 7 T using IVIM gradients. To assist with the interpretation of experimental data, the theoretical contribution of the IV BOLD component was calculated based on blood T_2 changes at different magnetic fields and echo times.

MATERIALS AND METHODS

Simulation of the IV Component in fMRI

The transverse relaxation rate of blood water is affected by the rapid exchange of water molecules between plasma and red blood cell interior and by the diffusion of plasma water in the presence of magnetic field gradients generated by deoxyhemoglobin sequestered within the red blood cells. In both cases, blood T_2 can be written as:

$$1/T_2 = A_0 + K(1 - Y)^2 \quad [1]$$

where Y is the fractional oxyhemoglobin content, A_o is a field-independent term and K scales quadratically with the magnetic field and is also dependent on the echo time used in a spin-echo measurement. Based on previous studies (17,18), it is generally thought that the exchange model dominates. Using the Luz-Meiboom exchange model (19), Eq. [1] can be further elaborated as:

$$1/T_2 = A_0 + \left[K_0\omega_0^2\left(1 - \frac{2\tau_{ex}}{\tau}\tanh\frac{\tau}{2\tau_{ex}}\right)\right](1 - Y)^2, \quad [2]$$

where K_o is a constant, ω_o is the magnetic field in frequency units, τ is the echo time (i.e., TE in imaging terminology) for the spin-echo measurement, and τ_{ex} is the average preexchange lifetime of water in the erythrocyte. For a CPMG experiment using an interpulse duration of 12 ms at 1.5 T (t_{180} in (20)), blood T_2 was reported to be ~127 and ~163 ms for Y = 0.6 and 0.7, respectively, which is similar to the T_2 value of 181 ms reported by Barth and Moser for Y = 0.72 (21). From these data, A_o and $K(=K_o\omega_o^2(1-(2\tau_{ex}/0.012)\tanh(0.012/2\tau_{ex})))$ were calculated to be 3.9 s^{-1} and 24.6 s^{-1} at τ of 12 ms and 1.5 T (20). Using these constants, apparent blood water T_2 for Y = 0.6 at higher magnetic fields and an echo time of 12 ms was estimated to be 11 ms at 7 T and 6 ms at 9.4 T. These extrapolated values are in relatively good agreement with ex vivo blood T_2 measured at 7 T (~12–15 ms (22,23)) and 9.4 T (5 ms (7)), suggesting that the parameters measured by Wright et al. (20) at 1.5 T are reasonable for estimating T_2 at different echo times, magnetic fields, and oxygenation levels. Thus, T_2 of blood water at a given magnetic field B_0 and spin echo time τ can be calculated by:

$$1/T_2 = 3.9 + 24.6(1 - Y)^2(B_0/1.5)^2 \times \left(1 - \frac{2\tau_{ex}}{\tau}\tanh\frac{\tau}{2\tau_{ex}}\right)\Big/\left(1 - \frac{2\tau_{ex}}{12}\tanh\frac{12}{2\tau_{ex}}\right). \quad [3]$$

Since the average exchange time, τ_{ex}, measured τ_{ex} of water was experimentally measured to range between 1 and 10 ms (1 ms by (15,17), 3–5 ms by (20), and 10 ms by (18)), simulations for τ_{ex} of 1, 5, and 10 ms were performed, with 1 and 10 ms being the extremes of τ_{ex}.

To calculate the IV contribution to the BOLD signal, the T_2 of tissue water ($T_{2(tissue)}$) and a venous blood volume fraction (α) was assumed to remain constant and Y was assumed to increase from 0.6 to 0.65 during visual stimulation (24). The effect of T_1 differences between tissue and blood water was ignored. The fractional intravascular BOLD signal from a voxel containing both tissue and blood at spin echo time TE can thus be written as:

$$\frac{\Delta S_{blood}}{S_{blood} + S_{tissue}} = \frac{\alpha\{e^{-TE/T_2(blood,\ stim)} - e^{-TE/T_2(blood,\ ctrl)}\}}{\alpha e^{-TE/T_2(blood,\ ctrl)} + (1 - \alpha)e^{-TE/T_2(tissue)}}, \quad [4]$$

where $T_{2(blood,ctrl)}$ and $T_{2(blood,stim)}$ are the T_2 values of blood water under control (with Y of 0.6) and stimulation (with Y of 0.65), which could be obtained from Eq. [3] for a given TE and B_0. For simulations, α was assumed to be 0.05 (25), and $T_{2(tissue)}$ values of gray matter water at 1.5, 3, 4, 7, and 9.4 T were taken to be 90 ms (26), 80 ms (27), 63 ms (28), 55 ms (23), and 40 ms (7), respectively. Potential partial-volume contributions from CSF and white matter in some voxels were ignored. These simulations also assumed that blood measured ex vivo was similar to in vivo.

FMRI Experiments

Normal volunteers (18–26 years old) participated in the study with informed consent in accordance with institutional guidelines. All fMRI studies were performed on a 4-T/90-cm (Oxford Instrument, Oxford, UK) or a 7-T/90-cm (Magnex Scientific, Abington, UK) magnet, driven by Varian's ^{unity}INOVA console (Palo Alto, CA) and equipped with Siemens gradient drivers. For GE acquisition, quadrature surface coils consisting of two overlapping circular loops (each of 12 cm inner diameter) were employed at both fields. For HSE acquisition, two-coil systems with actively detunable transmit and receiver coils were used. RF transmission was performed using a large TEM head coil at 4 T and a large half-volume coil with 12 × 16 cm dimension at 7 T, while signal detection was performed through a quadrature surface coil assembly (two overlapping circular loops of 6 cm diameter each). Manual and/or FASTMAP shimming were performed to optimize B_0 homogeneity.

fMRI was performed on a single 10-mm oblique slice along the calcarine fissure in the visual cortex. All images were acquired using single-shot EPI with a matrix size of 64 × 64 and 20 × 20 cm^2 field of view. The visual stimulus was 10 Hz flickering red/black light presented via goggles. Functional activation data were acquired in the presence of IVIM

gradients (10) (x, y, and z gradients were simultaneously turned on) with randomized *b*-values; for example, in a given study, where three different *b*-values were repeated, the *b*-values were 1, 100, 400, 100, 400, 1, 100, 400, 1, 100 s/mm^2, etc. Typically, 2–6 repeated measures for each *b*-value, on each subject, were made for all studies.

Hahn Spin-Echo BOLD fMRI

Hahn spin-echo EPI was acquired with paired unipolar gradients placed on both sides of the 180° refocusing pulse. To investigate the dependency of the IV BOLD component on TE, seven subjects at 4 T and four subjects at 7 T, were examined using a long TE (55–65 ms), and two subjects (six separate measures performed on each subject) participated in the short TE (32 ms) studies at each field. The HSE imaging parameters for long spin-echo time studies were: TR = 2 sec, 90° flip angle, TE = 65 ms (4 T) or 55 ms (7 T), intergradient pulse time (Δ) = 31 ms, gradient duration (δ) = 8.0 ms, and b = 1, 100, and 400 s/mm^2. These echo times were chosen to approximate the T_2 of parenchyma for optimal BOLD contrast. Spin-echo BOLD data, in the presence of S-T gradients at a short echo time (TE = 32 ms at both 4 and 7 T, chosen to increase sensitivity to intravascular contribution), were acquired using partial-Fourier *k*-space sampling (with eight additional *k*-space lines) with Δ = 15 ms, δ = 6 ms, and b = 1, 40, and 100 s/mm^2. This echo time was the shortest TE achievable in the presence of the S-T gradients. A two-epoch paradigm of 10–**10**–15–**10**–15 images (bold case indicates images obtained during flashing lights) was acquired.

The potential contributions from inherent T_2^* weighting due to EPI acquisition was evaluated for the HSE BOLD fMRI images using different echo times (TE = 20, 40, 60, 80, 100 ms) at 7 T (n = 3) *without* IVIM gradients (but leaving a pair of crushers around the 180° refocusing pulse). Partial Fourier *k*-space sampling with 11 additional *k*-space lines was used. Additionally, in-flow effect in the randomly oriented *large* blood vessels, if it exists, could in principle be suppressed by S-T gradients. To evaluate the in-flow effect from randomly oriented *large* vessels to the HSE BOLD signal in the presence of IVIM gradients, fMRI data (TE = 55 ms) were collected with a longer TR of 4 sec at 7 T and compared with those collected with TR of 2 sec in the same subjects (n = 4).

Gradient-Echo BOLD fMRI

Gradient-echo EPI was acquired with a pair of S-T gradients placed after the excitation pulse. The GE imaging parameters were: TR = 2 sec, 90° flip angle, TE = 80 ms (4 T) or 55 ms (7 T), Δ = 21 ms, δ = 20 ms, and b = 1, 20, 40, 100, 200, 400, and 500 s/mm^2. A three-epoch paradigm of 10–**10**–10–**10**–10–**10**–10 images was used. Five subjects participated in the gradient-echo studies at each field.

FMRI Data Analysis

Data analysis employed programs written in PV-WAVE (Visual Numerics, Houston, TX) and STIMULATE software. fMRI data were evaluated for head motion by displaying the consecutively acquired images as a repeating movie. The data were discarded if apparent motion was detected. No motion correction for coregistration was used across data obtained using different *b*-values. This decision was based on the fact that data analysis was performed on a large region of interest (ROI) containing many voxels; hence, the requirement for coregistration was not stringent.

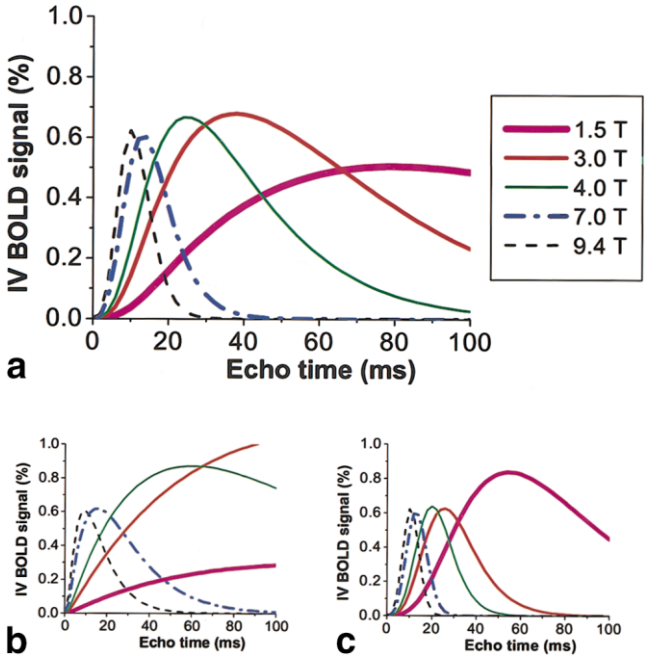

FIG. 1. Simulation of the intravascular BOLD signal change, $\Delta S_{blood}/(S_{blood}+S_{tissue})$, as a function of echo time for a Hahn (single) spin echo at 1.5, 3, 4, 7, and 9.4 T. A venous blood volume of 0.05, no stimulus-evoked blood volume change, and an increase in venous oxygenation level from 0.6 to 0.65 during stimulation were assumed. The T_2 values of blood water at different field strengths and as a function of echo time were calculated from experimental data reported by Wright et al. at 1.5 T (20), as described in Materials and Methods. Simulations for τ_{ex} of 5 ms (**a**), 1 ms (**b**), and 10 ms (**c**) were performed. The overall patterns of the curves at both extremes of exchange times were similar.

Cross-correlation (CC) maps were computed to assess data quality. Images from the control and stimulated periods were averaged. Percent changes were calculated in the following manner. In a typical fMRI session, the first visual stimulation was acquired using b = 1 s/mm^2. A CC activation map was calculated for this dataset (CC threshold of 0.4 for GE data and 0.3 for HSE data, corresponding to P = 0.008 and 0.02, respectively). Percent changes for the remaining datasets were calculated using this map as a mask. In other words, an ROI (of an irregular shape) was defined as consisting of all the pixels that were classified as activated in the b = 1 s/mm^2 map for each subject. Subsequently, in each subject signal intensity changes were calculated for this ROI at the different *b*-values, *without* any classification of pixels as "activated" or not. To avoid bias, the dataset used to generate the mask (b = 1 s/mm^2) was excluded from further analysis. Percent changes were normalized to those with a *b*-value of 1 s/mm^2 for each subject, averaged across subjects and

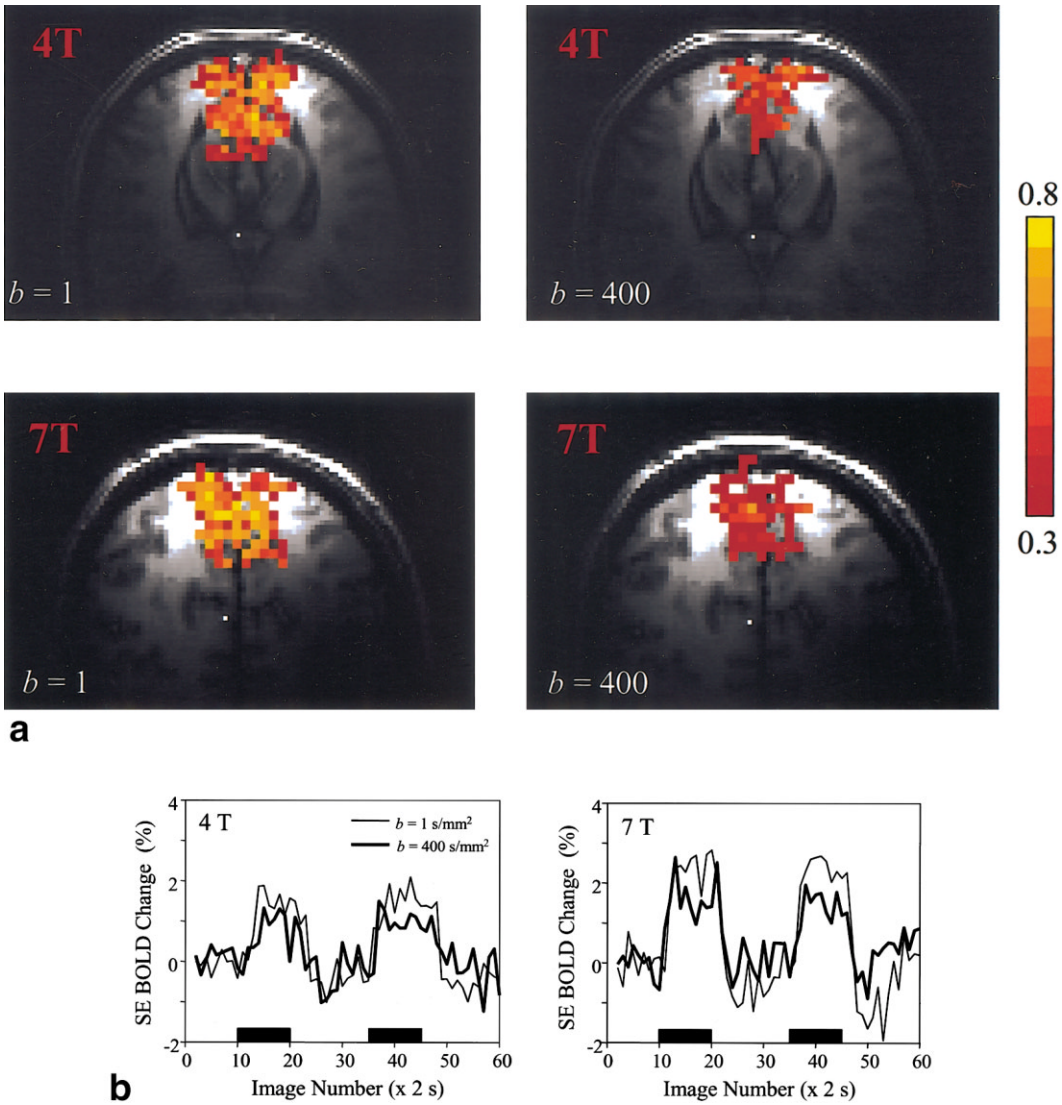

FIG. 2. Representative single-scan, HSE BOLD fMRI at 4 and 7 T. Cross-correlation (CC) maps (**a**) and time courses (**b**) obtained with b = 1 and 400 s/mm^2 at 4 and 7 T. The color scale indicates the CC values of 0.3–0.8. The number of activated pixels decreases with increasing b-values at a given statistical threshold. Spin echo time was 65 ms at 4 T and 55 ms at 7 T. Boxes under time courses indicate stimulation duration.

plotted as a function of b-value. All reported values were mean ± standard deviation and error bars on graphs were standard errors of the means.

RESULTS

Simulation of the IV Component in Spin-Echo fMRI

Percent change of the spin-echo BOLD signal due to the IV component is shown as a function of echo time at 1.5, 3, 4, 7, and 9.4 T in Fig. 1. The overall shapes of the curves do not substantially change for τ_{ex} of 1, 5, and 10 ms, although the details of the TE dependence were different. For the conclusions reached in this article, the differences are immaterial since all simulations for different τ_{ex} values predicted a much larger and substantial blood contribution at 4 T compared to 7 T at a TE of 32 ms, and small blood contributions at TE = 55 ms for 7 T and 65 ms for 4 T. In these simulations, the venous volume fraction of 5% is applicable for a large ROI or the entire brain. However, a venous blood volume fraction may be larger than 5% in some pixels containing large vessels. Equation [4] assumed that α does not change with increased neural activity. Changing the blood-volume fraction (α in Eq. [4]) and the oxygenation level (Y in Eq. [3]), however, does not change the shape of the curves; it only affects the amplitude of the IV contribution. Similarly, the effect of T_1 differences between tissue and blood water was ignored in Eq. [4]. This T_1 difference will increase the blood effect relative to tissue when TR is not sufficiently long to allow close to full relaxation. However, this will not affect the TE

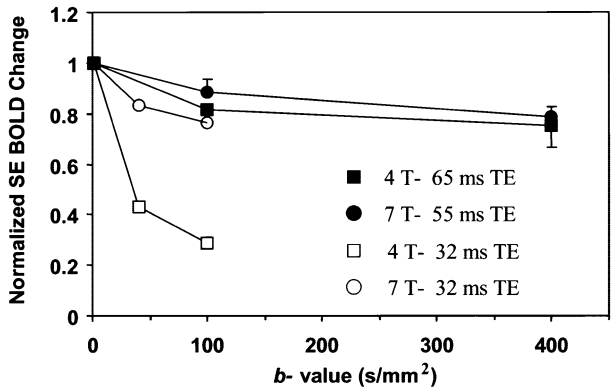

FIG. 3. Normalized HSE BOLD percent changes as a function of *b*-value for short and long echo times at 4 and 7 T. Percent changes were normalized to the BOLD change at $b = 1$ s/mm^2 for each subject and averaged for each field. Closed squares and circles indicate HSE data with TE of 65 ms at 4 T (n = 7) and with TE of 55 ms at 7 T (n = 4), respectively. Open squares and circles indicate HSE data with TE of 32 ms at 4 and 7 T, respectively, for two subjects at each field (six repeated measurements were made for each subject). Error bars = SEM. For long TE, the attenuation was not statistically different between 4 and 7 T ($P > 0.05$).

dependence of the curves displayed in Fig. 1; it will only affect the amplitude of the IV contribution.

Although apparent water exchange time τ_{ex} can impact the exact shape of the curve, especially at 1.5 and 3 T, the general patterns as a function of echo time remain intact. The overall shapes of the simulated curves were largely invariant with respect to τ_{ex} from 1–10 ms. The general features of these simulations are that IV contributions are echo time-dependent and diminish with increasing echo time for values exceeding the blood T_2. Note that for the spin-echo times used in the plots (Fig. 1), the blood contribution is increasing with echo time at 1.5 T, whereas at 4–9.4 T it is decreasing after reaching a maximum. In particular, at the higher field strength of 7 and 9.4 T, the onset of the IV signal decrease occurs at a shorter echo time, as expected.

Spin-Echo BOLD fMRI

Figure 2 shows representative HSE BOLD images and time courses with long echo times at 4 (TE = 65 ms) and 7 T (TE = 55 ms) obtained in the presence of IVIM gradients. HSE BOLD responses were robustly detected in the visual cortex along the calcarine fissure. The average HSE BOLD responses for $b = 1$ s/mm^2 were 1.4 ± 0.4% (TE = 65 ms, n = 7) at 4 T and 1.9 ± 0.5% (TE = 55 ms, n = 4) at 7 T (see time courses for single-subject data). The average HSE BOLD changes at TE of 32 ms were 0.8% at 4 T (n = 6) and 1.1% at 7 T (n = 6). Higher statistical values (yellow pixels) were observed at 7 T compared to 4 T, suggesting a higher contrast-to-noise ratio (CNR) at the higher field. The areas of activation maps for a fixed cross-correlation statistical threshold decreased with increasing *b*-values, presumably because of decreased signal-to-noise ratio (SNR), and decreasing CNR due to both increased image-to-image fluctuations and diminished BOLD signal changes associated with blood. SNR is reduced because IVIM gradients result in signal loss in tissue due to diffusion effects (a *b*-value of 400 s/mm^2 decreases tissue signal by ~30%). In the presence of the IVIM gradients, image-to-image signal fluctuations increased due to increased sensitivity to motions, including pulsation in the brain associated with heartbeat and respiration, resulting in a decrease in CNR. Consequently, the activation maps obtained with the same statistical threshold could not be justified for evaluating the effect of *b*-value on percent signal intensity changes. Rather, as described in Materials and Methods, an ROI was independently defined and the same ROI was used to obtain the signal changes for all *b*-value data without any classification of pixels into activated or nonactivated groups.

The *b*-value dependence for the HSE BOLD data in the presence of IVIM gradients, averaged for all subjects, is illustrated in Fig. 3 for an echo time of 32 ms at 4 and 7 T, and for echo times of 65 and 55 ms for 4 and 7 T, respectively. At a TE of 32 ms, the IVIM gradients induced a significant loss in percent BOLD signal change ($\Delta S/S$) at 4 T but had a lesser impact at 7 T, in agreement with the theoretical predictions (Fig. 1). At the longer echo times the reduction in BOLD percent changes at a *b*-value of 100 s/mm^2 was significantly less at both fields, but relatively larger at 4 T compared to 7 T, again consistent with predictions (Fig. 1). Minor additional attenuation was observed at these long echo times as *b*-value was increased up to 400 s/mm^2. The large difference seen in the echo time dependence of the suppression of $\Delta S/S$ due to IVIM gradients is consistent with the IV BOLD modeling (Fig. 1). Since the 32 ms echo time is ~3 times the T_2 of venous blood at 7 T, but similar to the T_2 of venous blood at 4 T (31 ms at Y of 0.6 based on Eq. [2]), the IV contribution is small at 7 T but significantly larger at 4 T for this echo time. Setting an echo time much longer than venous blood T_2 would reduce the IV contribution.

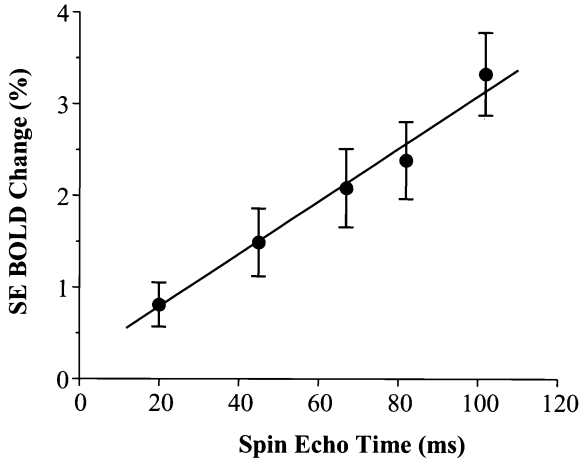

FIG. 4. HSE BOLD percent changes as a function of echo times at 7 T (n = 3). The data are best fitted by a linear equation where BOLD percent changes = 0.21 + 0.029 × TE (in ms). Error bars = SEM.

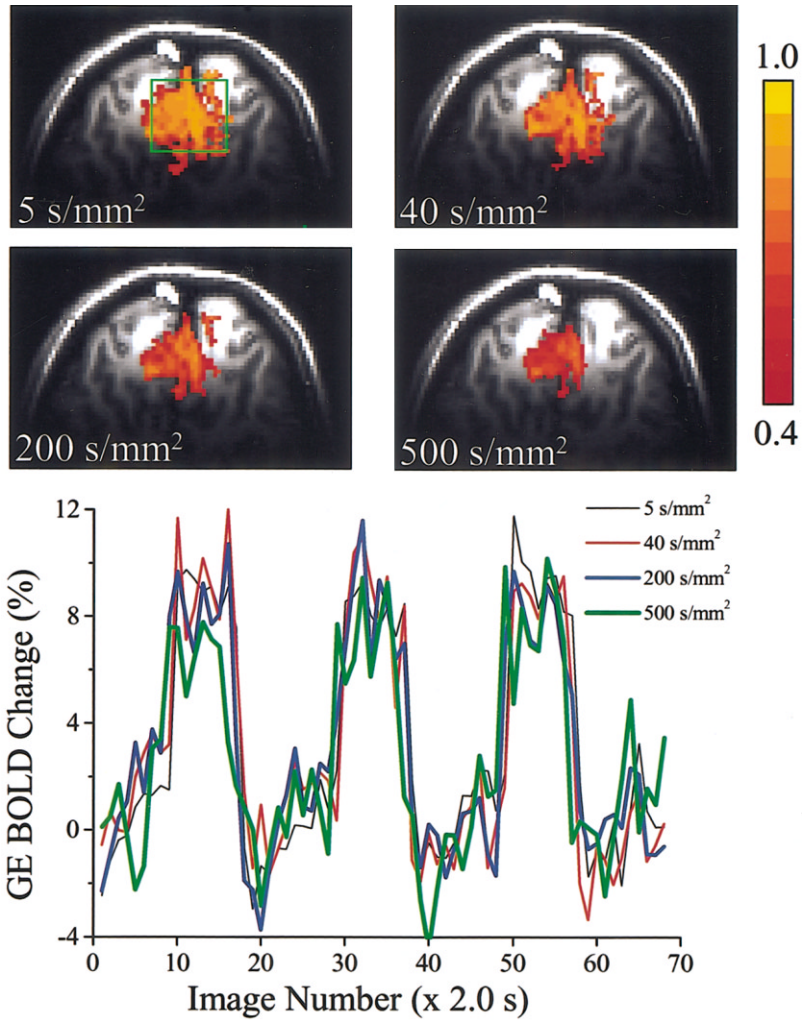

FIG. 5. GE BOLD maps obtained at 4 T (TE = 80 ms) and time courses for four representative *b*-values. Functional maps for the four *b*-values from a single scan were displayed with the same minimum cross-correlation value of 0.4. The color scale indicates the CC values of 0.4–1.0. The percent changes, obtained using the same ROI (shown in a green rectangle) without a mask remain relatively constant.

The intercept of ΔS/S vs. echo time is a measure of all non-T_2 effects, which can arise from the T_2^* contribution of the EPI acquisition as well as from in-flow. Figure 4 displays a plot of HSE percent changes vs. echo time, averaged for all subjects in an ROI covering the primary visual area. Extrapolating the HSE BOLD percent change to zero intercept demonstrated that the non-T_2 effects were minimal at 7 T (0.2% out of a total 1.8% at TE = 55 ms). The effect of short and long TR (2 and 4 sec) was also evaluated at 7 T in order to assess the in-flow contribution. The decrease in ΔS/S by IVIM gradients was not statistically different between HSE fMRI data obtained with TR = 2 and 4 sec at 7 T (data not shown). These non spin-echo contributions to ΔS/S are expected to be less at 4 T because of the shorter T_1 and longer T_2^* values at a lower field.

Gradient-Echo BOLD fMRI

A representative GE BOLD study in the presence of IVIM gradients at 4 T without signal averaging is shown in Fig. 5 for an echo time of 80 ms. The average GE BOLD responses for b = 1 s/mm^2 were 7.0 ± 1.0% at 4 T (TE = 80 ms, n = 5), and 5.4 ± 1.3% at 7 T (TE = 55 ms, n = 5). Note that T_2^* of gray matter water at 4 and 7 T were ~35 and ~25 ms, respectively (23). The areas of the cross-correlation activation maps decreased with increasing *b*-values, as expected. Time courses were obtained from the same ROI across different *b*-values, as previously described. Percent changes remained relatively constant as *b*-values increased, but baseline signal fluctuation increased due to decreased SNR and increased image-to-image signal fluctuations (time courses in Fig. 5). Normalized percent changes at 4 T (echo-time = 80 ms) and 7 T (echo time = 55 ms), from all five subjects, at each field, are plotted as a function of *b*-value (Fig. 6). The percent changes for these long echo times at both fields were not significantly attenuated by IVIM gradients.

Our finding differs from similar studies conducted at 1.5 T, where the GE BOLD signals were eliminated or markedly (70%) reduced (12,13) by IVIM gradients, suggesting the GE BOLD signals at 1.5 T (with echo times approximating tissue T_2^*) arose predominantly from IV effects associated with large venous blood vessels. Similar GE BOLD studies at 3 T showed approximately 60% attenuation by IVIM gradients (b = 200 s/mm^2) (29). These differences are consistent with field-dependent effects which predicted a rapid decrease of blood T_2 and T_2^* with increasing field strength (Fig. 1).

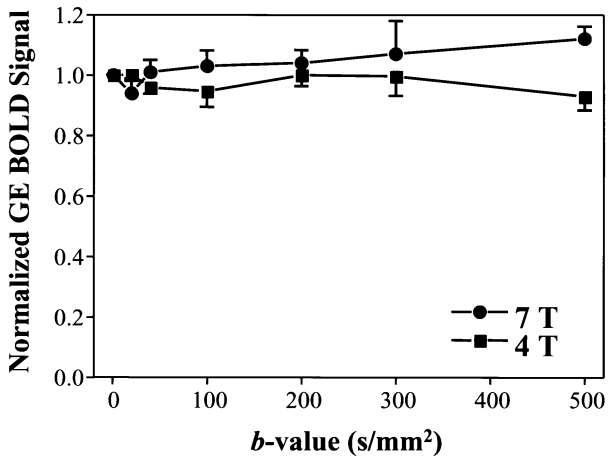

FIG. 6. Normalized GE BOLD changes as a functional of *b*-values at 4 and 7 T (n = 5 subjects at each field). GE BOLD changes were normalized for each subject and averaged across subjects for each field. Gradient-echo times used here were 55 ms at 7 T and 80 ms at 4 T. Error bars = SEM.

DISCUSSION

BOLD Percent Changes Between 4 T and 7 T

A quantitative comparison of stimulation-evoked BOLD percent changes at the two different magnetic fields was *not* attempted in this work because different subjects and imaging slices were used. Quantitative comparisons among different magnetic fields require at least the use of same subjects and virtually identical imaging slices, as was done previously for a gradient-echo BOLD fMRI study (23). A systematic field-dependent comparison of ΔR_2 in the same subjects at 4 and 7 T was performed separately. These studies showed that, when the blood effects were suppressed, $\Delta S/S$ for HSE fMRI increases near quadratically (2.6-fold), going from 4 T to 7 T (30).

In this study, the effects of the IVIM gradients were normalized to the lowest *b*-value for each subject before intersubject averaging in order to avoid variations due to intersubject differences in magnitude of the BOLD effect. Consequently, quantitative comparisons could be made with respect to the effect of the IVIM gradients on the BOLD signal changes.

Specificity of High-Field fMRI Signals

Because of the role played by the vasculature, the specificity of BOLD-based fMRI maps can be significantly degraded relative to the actual areas of increased blood flow and oxygen consumption that accompany elevated neuronal activity. Deoxyhemoglobin changes initially occur at the area of increased neuronal activity and subsequently propagate down the venous vasculature, including large draining veins that are distant from the site of elevated neuronal activity (31–33). Dilution by blood draining from "inactive" areas should ultimately diminish this nonspecific draining-vein effect and thus limit its spatial extent; however, before this occurs substantial nonspecific and false "activation" can be generated. Therefore, it is important to minimize both IV and EV contributions induced by draining veins. The data presented here demonstrate that this can be achieved by using Hahn spin-echo acquisitions at high magnetic fields.

A spin-echo acquisition scheme can improve the spatial specificity of BOLD fMRI by suppressing the EV effect from large veins. Spin-echo BOLD contains an EV component *associated only with small-diameter blood vessels* and an IV component due to blood T_2 changes that arise from alterations in the fractional content of deoxyhemoglobin (see review article (9)). The blood vessels that contribute to the EV BOLD effect in HSE data are the water molecules that have sufficiently large net displacements (during the echo time TE) to dynamically average the magnetic field gradients generated by deoxyhemoglobin in blood. This effect is dependent on "diffusion" time, venous oxygenation level, magnetic field strength, and vessel radius (1,2,34). Deoxyhemoglobin containing vessels of different sizes would have different amounts of irreversible dynamic averaging components, resulting in a bell-shaped distribution curve for HSE signal changes vs. blood vessel radius or a continuous and increasingly steeper enhancement of $(\Delta S/S)_{HSE}/(\Delta S/S)_{GE}$ with decreasing vessel radius (1,2). A population of vessels with radii less than ~5–8 μm (with maximal effects at about half these radii) were found to contribute to HSE signals when the susceptibility-induced frequency difference between cylinders representing the blood vessels and their surrounding spaces was 64 to 32 Hz, respectively (1).

However, since the HSE BOLD signal also contains, in principle, an IV component, it can arise from both small and large vessels as long as this IV component is significant. The IV contribution from large veins is expected to be markedly reduced at high magnetic fields (Fig. 1) for HSE BOLD signals at echo times corresponding to tissue T_2 and, in the case of 7 T, at echo times even shorter than tissue T_2. This is ascribed to the fact that the apparent T_2 of venous blood decreases faster than that of tissue with increasing magnetic fields. For example, the apparent T_2 of venous blood at O_2 saturation Y of 0.6 is 12–15 ms at 7 T (22,23), while T_2 of gray matter is 50–55 ms at 7 T (35). Therefore, the IV component can be selectively reduced by increasing echo times at high fields. At low fields, on the other hand, the apparent T_2 of venous blood is quite long (e.g., 90–180 ms depending on Y at 1.5 T (20,21)) and comparable or substantially longer than tissue T_2 (~90 ms in gray matter; (26)). Therefore, there is a significant IV signal when TE is set to tissue T_2 at low fields. Furthermore, the IV contribution can*not* be reduced by increasing echo times at low fields if the blood T_2 is comparable to or longer than tissue T_2 (Fig. 1), which is the case for 1.5 T.

The small suppression of BOLD signal change by IVIM gradients, at longer echo times approximating or exceeding tissue T_2 at 4 T, may appear to contradict an earlier study by Menon et al. (36) using spin-echo BOLD fMRI with a relatively long TE of 70 ms at 4 T. In that study, the number of activation pixels decreased up to 40% with b = 200 s/mm^2. However, the number of activated pixels (not percent changes in an ROI) was evaluated as a function of *b*-values. Since the SNR and CNR decreases with increasing *b*-value, the number of activated pixels at a given statistical threshold is expected to decrease, irrespective of whether there is an IV contribution (e.g., (7)). Thus, the

number of activated pixels cannot be used for evaluating the IV and EV contribution to the BOLD response. Percent signal changes in a predefined ROI were therefore examined in this study.

GE fMRI data should behave similarly as the HSE results with respect to blood contribution; the IV contribution should be less at longer TE and/or at higher fields. The suppression of stimulus-evoked BOLD signal changes by the IVIM gradients at 4 T and TE of 80 ms should be very small and approximately the same as those observed for 7 T at 55 ms or even at 30 ms echo time (Fig. 1). This is in agreement with the experimental data (Figs. 3, 6) and results previously reported with GE BOLD studies at 7 T (23).

IVIM Gradients

Significant echo time and *b*-value dependent suppression by IVIM gradients were observed, documenting that there is indeed a field-dependent "intravascular" blood component in the BOLD signal changes in the human brain during visual stimulation. However, the extent to which IVIM gradients can suppress IV signal is dependent on vessel sizes and remains controversial (37–39). BOLD signal changes, detected even in the presence of the highest *b*-values attained in this study, may still contain some IV contributions. However, as discussed below, our data suggest that this potential residual blood contribution is small.

At 4 T and TE of 32 ms, 75% of the stimulus-invoked HSE BOLD signal changes can be suppressed by the IVIM gradients ($b = 100$ s/mm^2) (Fig. 3). This means that *at least* this fraction can be ascribed to blood-related effects at that specific echo time and field strength; the remaining 25% of the HSE BOLD signal change then defines the *upper limit* of the *residual* blood effects that *may not* have been suppressed by the IVIM gradients at a *b*-value of 100 s/mm^2. Since the mechanisms by which IVIM gradients suppress the blood signals are field-independent, this upper limit also applies to the 7 T data. However, our simulations (Fig. 1) suggest that the contribution of this possible *residual* blood effect is likely to be significantly smaller than 25% at 7 T with an echo time of 32 ms (Fig. 1). Similarly, it can be concluded that possible *residual* blood contributions to BOLD signal changes at 4 and 7 T at echo times of 65 ms and 55 ms, respectively, must also be significantly smaller than 25% of the stimulus-evoked signal changes.

Superficially, this conclusion may appear to contradict the data on the effect of IVIM gradients in anesthetized rat brains in which an intravascular perfluorocarbon (PFC) compound was administered as a blood substitute (37,38). In these two studies it was demonstrated that PFC blood-substitute in the veins cannot be completely suppressed using IVIM gradients with *b*-value up to 500 s/mm^2. However, the difference can be explained based on diffusion constants of blood water and the much larger PFC molecule. The diffusion constant of blood water is ~2.5 times greater than that of brain tissue water which is $\sim 0.8 \times 10^{-3}$ mm^2/s. Therefore, at *b*-values of 100 and 400 s/mm^2, blood contribution due to diffusion alone (without considering flow and IVIM mechanisms) would be suppressed by 22% and 63%, respectively, while tissue signals are reduced by 10% and 33%, respectively. In contrast, the decrease in PFC signals with increasing *b*-value is only flow- or IVIM-related, not diffusion-related, because of its extremely small diffusion constant. The diffusion component can be ignored for the PFC signals in the presence of IVIM gradients. On the other hand, at a *b*-value of 400 s/mm^2, this diffusion effect alone would eliminate more than half of the blood water signals.

A small decrease in the overall apparent diffusion coefficient (ADC) in the brain, associated with increased neural activity has been reported (40). At a given *b*-value, the ADC decrease induced by neuronal activity will also lead to a small underestimation of the blood contribution in the data presented here. This effect, however, is expected to be field-independent and virtually TE-independent due to the small apparent change in ADC. Therefore, the stimulus-evoked ADC changes do not alter the conclusions presented in this article regarding relative contribution of blood at 4 vs. 7 T or at different echo times. Clearly, there is a large effect of the IVIM gradients at 4 T with short echo times and this effect decreases significantly with increasing magnetic field or longer echo times.

CONCLUSION

Decreased IV contributions were observed at 7 T relative to 4 T, and the relative contributions of the IV signals for the two magnetic fields were echo time-dependent and are consistent with theoretical predictions. These data also indicate that the signal changes associated with brain function, detected with HSE BOLD mechanism at both 4 T and 7 T with echo times equal to or larger than the tissue T_2, originate largely from an EV BOLD effect from the microvasculature.

ACKNOWLEDGMENTS

We thank Drs. Peter Andersen, Tommy Vaughan, and Hellmut Merkle for hardware support.

REFERENCES

1. Ogawa S, Menon RS, Tank DW, Kim S-G, Merkle H, Ellermann JM, Ugurbil K. Functional brain mapping by blood oxygenation level-dependent contrast magnetic resonance imaging. Biophys J 1993;64:800–812.
2. Boxerman JL, Hamberg LM, Rosen BR, Weisskoff RM. MR contrast due to Intravascular magnetic susceptibility perturbations. Magn Reson Med 1995;34:555–566.
3. Duong TQ, Silva AC, Lee S-P, Kim S-G. Functional MRI of calcium-dependent synaptic activity: cross correlation with CBF and BOLD measurements. Magn Reson Med 2000;43:338–392.
4. Haacke E, Lai S, Yablonskiy D, Lin W. In vivo validation of the BOLD mechanism: A review of signal changes in gradient echo functional MRI in the presence of flow. Int J Imag Syst Technol 1995;6:153–163.
5. Ugurbil K, Hu X, Chen W, Zhu XH, Kim S-G, Georgopoulos A. Functional mapping in the human brain using high magnetic fields. Philos Trans R Soc Lond B 1999;354:1195–1213.
6. Bandettini PA, Wong EC, Jesmanowicz A, Hinks RS, Hyde JS. Spin-echo gradient-echo EPI of human brain activation using BOLD contrast: a comparative study at 1.5T. NMR Biomed 1994;7:12–20.
7. Lee S-P, Silva AC, Ugurbil K, Kim S-G. Diffusion-weighted spin-echo fMRI at 9.4 T: microvascular/tissue contribution to BOLD signal change. Magn Reson Med 1999;42:919–928.

8. Oja JME, Gillen J, Kauppinen RA, Kraut M, van Zijl PCM. Venous blood effects in spin-echo fMRI of human brain. Magn Reson Med 1999;42: 617–626.
9. Ogawa S, Menon RS, Kim S-G, Ugurbil K. On the characteristics of functional magnetic resonance imaging of the brain. Annu Rev Biophys Biomol Struct 1998;27:447–474.
10. Stejskal EO, Tanner JE. Spin diffusion measurements: spin echoes in the presence of a time-dependent field gradient. J Chem Phys 1965;42: 288–292.
11. LeBihan D, Breton E, Lallemand D, Aubin ML, Vitnaud J, Laval-Jeantet M. Separation of diffusion and perfusion in intravoxel incoherent motion MR imaging. Radiology 1988;168:497–505.
12. Song AW, Wong EC, Tan SG, Hyde JS. Diffusion-weighted fMRI at 1.5T. Magn Reson Med 1996;35:155–158.
13. Boxerman JL, Bandettini PA, Kwong KK, Baker JR, Davis TL, Rosen BR, Weisskoff RM. The intravascular contribution to fMRI signal change: Monte Carlo modeling and diffusion-weighted studies in vivo. Magn Reson Med 1995;34:4–10.
14. Hoogenraad FG, Pouwels PJ, Hofman MB, Reichenbach JR, Sprenger M, Haacke EM. Quantitative differentiation between BOLD models in fMRI. Magn Reson Med 2001;45:233–246.
15. Thulborn KR, Waterton JC, Mattews PM, Radda GK. Oxygenation dependence of the transverse relaxation time of water protons in whole blood at high field. Biochem Biophys Acta 1982;714:265–270.
16. Lee S-P, Silva AC, Kim S-G. Comparison of diffusion-weighted high-resolution CBF and spin-echo BOLD fMRI at 9.4 T. Magn Reson Med 2002;47:736–741.
17. Meyer M, Yu O, Eclancher B, Grucker D, Chambron J. NMR relaxation rates and blood oxygenation level. Magn Reson Med 1995;34:234–241.
18. Bryant R, Marill K, Blackmore C, Francis C. Magnetic relaxation of water and water clots. Magn Reson Med 1990;13:133–144.
19. Luz Z, Meiboom S. Nuclear magnetic resonance study of the protolysis of trimethyammonium ion in aqueous solution—order of the reaction with respect to solvent. J Chem Phys 1963;39:366–370.
20. Wright GA, Hu BS, Macovski A. Estimating oxygen saturation of blood in vivo with MR imaging at 1.5 T. J Magn Reson Imag 1991;1:275–283.
21. Barth M, Moser E. Proton NMR relaxation times of human blood samples at 1.5 T and implications for functional MRI. Cell Mol Biol 1997; 43:783–791.
22. Ogawa S, Lee TM, Barrere B. Sensitivity of magnetic resonance image signals of a rat brain to changes in the cerebral venous blood oxygenation. Magn Reson Med 1993;29:205–210.
23. Yacoub E, Shmuel A, Pfeuffer J, van de Moortele P-F, Adriany G, Andersen P, Vaughan JT, Merkle H, Ugurbil K, Hu X. Imaging brain function in humans at 7 Tesla. Magn Reson Med 2001;45:588–594.
24. Kim S-G, Rostrup E, Larsson HBW, Ogawa S, Paulson OB. Simultaneous measurements of CBF and CMRO2 changes by fMRI: significant increase of oxygen consumption rate during visual stimulation. Magn Reson Med 1999;41:1152–1161.
25. Phelps M, Grubb RJ, Ter-Pogossian M. Correlation between PaCO2 and regional cerebral blood volume by x-ray fluorescence. J Appl Physiol 1973;35:274–280.
26. Breger RK, Rimm AA, Fischer ME, Papke RA, Haughten VM. T_1 and T_2 measurements on a 1.5 Tesla commercial imager. Radiology 1989;171: 273–276.
27. Wansapura JP, Holland SK, Dunn RS, Ball WS. NMR relaxation times in human brain at 3.0 Tesla. J Magn Reson Imag 1999;9:531–538.
28. Jezzard P, Duewell S, Balaban RS. MR relaxation times in human brain—measurement at 4 T. Radiology 1996;199:773–779.
29. Song AW, Wong EC, Jezmanowicz A, Tan SG, Hyde JS. Diffusion weighted fMRI at 1.5T and 3T. In: Proc 3rd Scientific Meeting ISMRM, 1995, Nice, France. p 457.
30. Yacoub E, Duong TQ, van de Moortele PF, Lindquist M, Adriany G, Kim SK, Hu X, Ugurbil K. Spin echo fMRI in humans using high spatial resolutions and high magnetic fields. Magn Reson Med 2003;49:655–664.
31. Lai S, Hopkins AL, Haacke EM, Li D, Wasserman BA, Buckley P, Friedman H, Meltzer H, Hedera, Friedland R. Identification of vascular structures as a major source of signal contrast in high resolution 2D and 3D functional activation imaging of the motor cortex at 1.5T: preliminary results. Magn Reson Med 1993;30:387–392.
32. Duong TQ, Kim D-S, Ugurbil K, Kim S-G. Spatio-temporal dynamics of the BOLD fMRI signals in cat visual cortex: toward mapping columnar structures using the early negative response. Magn Reson Med 2000; 44:231–242.
33. Duong TQ, Kim D-S, Ugurbil K, Kim S-G. Localized blood flow response at sub-millimeter columnar resolution. Proc Natl Acad Sci USA 2001;98:10904–10909.
34. Kennan RP, Zhong J, Gore JC. Intravascular susceptibility contrast mechanisms in tissues. Magn Reson Med 1994;31:9–21.
35. Bartha R, Michaeli S, Merkle H, Adriany G, Andersen P, Chen W, Ugurbil K, Garwood M. In vivo 1H2O T2 measurement in the human occipital lobe at 4T and 7T by Carr-Purcell MRI: detection of microscopic susceptibility contrast. Magn Reson Med 2002;47:742–750.
36. Menon RS, Hu X, Adriany G, Andersen P, Ogawa S, Ugurbil K. Comparison of SE-EPI, ASE-EPI and conventional EPI applied to functional neuroimaging: the effect of flow crushing gradients on the BOLD signal. Proc Soc Magn Reson 1994;2:622.
37. Neil J, Ackerman J. Detection of pseudodiffusion in rat brain following blood substitution with perfluorocarbon. J Magn Reson 1992;97:194–201.
38. Duong TQ, Kim S-G. In vivo MR measurements of regional arterial and venous blood volume fractions in intact rat brain. Magn Reson Med 2000;43:392–402.
39. Henkelman RM, Neil JJ, Xiang Q-S. A quantitative interpretation of IVIM measurements of vascular perfusion in the rat brain. Magn Reson Med 1994;32:464–469.
40. Darquié A, Poline J-B, Poupon C, Saint-Jalmes H, LeBihan D. Transient decrease in water diffusion observed in human occipital cortex during visual stimulation. Proc Natl Acad Sci USA 2001;98:9391–9395.